

Effective mass suppression upon complete spin-polarization in an isotropic two-dimensional electron system

T. Gokmen, Medini Padmanabhan, K. Vakili, E. Tutuc, and M. Shayegan
Department of Electrical Engineering, Princeton University, Princeton, NJ 08544

(Dated: October 25, 2018)

We measure the effective mass (m^*) of interacting two-dimensional electrons confined to a 4.5 nm-wide AlAs quantum well. The electrons in this well occupy a single out-of-plane conduction band valley with an isotropic in-plane Fermi contour. When the electrons are partially spin polarized, m^* is larger than its band value and increases as the density is reduced. However, as the system is driven to full spin-polarization via the application of a strong parallel magnetic field, m^* is suppressed down to values near or even below the band mass. Our results are consistent with the previously reported measurements on wide AlAs quantum wells where the electrons occupy an in-plane valley with an anisotropic Fermi contour and effective mass, and suggest that the effective mass suppression upon complete spin polarization is a genuine property of interacting two-dimensional electrons.

PACS numbers:

As the density of an interacting two-dimensional electron system (2DES) is reduced, the interaction strength characterized by the ratio r_s of the Coulomb energy to Fermi energy, is enhanced. In low disorder, dilute 2DESs the ground state properties are dominated by the electron-electron interaction [1]. In the Fermi liquid theory, interactions modify the Fermi liquid parameters [2] and renormalize the effective mass (m^*) and the spin susceptibility ($\chi^* \propto g^* m^*$) of the 2DES, where g^* is the Lande g -factor. In particular, χ^* and m^* are expected to be larger than the band values (χ_b and m_b) for large r_s [3, 4, 5, 6, 7, 8, 9, 10]. Indeed, enhancements of χ^* and m^* at large r_s are observed in various 2DESs [11, 12, 13, 14, 15, 16, 17, 18, 19, 20, 21, 22, 23, 24, 25]. However, in 2DESs occupying wide AlAs quantum wells (QWs) an unexpected trend is observed as the system becomes fully spin polarized: m^* is suppressed and falls to values near or below m_b even for r_s values up to 21 [26]. A subsequent study in similar samples [27] revealed that the mass suppression disappears when the electrons occupy two conduction-band valleys, signaling that the mass suppression is unique to single-component (fully spin and valley polarized) systems.

Here we report measurements of m^* in the partially and fully spin polarized regime as a function of density in a 2DES where the electrons are confined to a 4.5 nm-wide AlAs QW. This 2DES is different from the 2DESs used in Ref. [26] in two important aspects: it has a very *small* layer thickness (< 4.5 nm) and an *isotropic* effective mass. Bulk AlAs has three equivalent, ellipsoidal conduction band valleys at the X-points of the Brillouin zone with longitudinal and transverse effective masses, $m_l=1.05$ and $m_t=0.205$ (in units of the free electron mass) [28, 29, 30, 31]. In samples of Ref. [26], the electrons are confined to either an 11 nm- or 15 nm-wide AlAs QW and occupy one of the two in-plane valleys with an anisotropic Fermi contour and anisotropic band masses equal to 0.205 and 1.05, leading to $m_b = \sqrt{m_l m_t} = 0.46$.

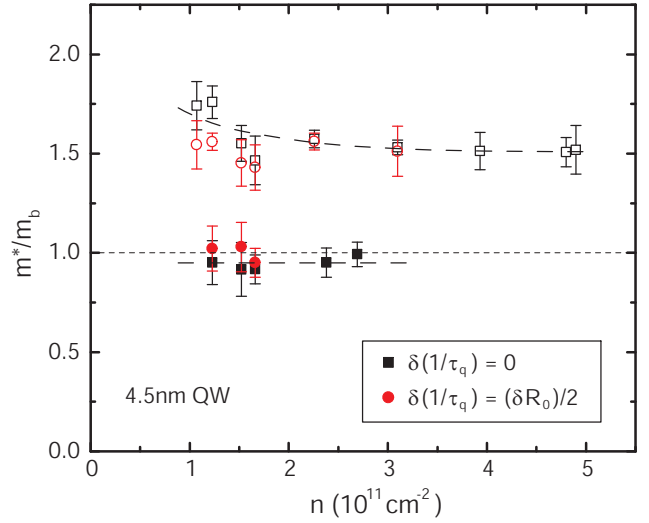


FIG. 1: (Color online) Effective mass, normalized to the band mass, measured as a function of density for a 2DES confined to a 4.5 nm-wide AlAs quantum well. Open and closed symbols represent m^* measured in partially and fully spin-polarized 2DESs, respectively. Black and red points correspond to m^* values deduced either assuming a constant quantum lifetime τ_q or that the relative temperature-dependence of τ_q is half the size of the relative temperature-dependence of the background resistance, respectively. Each data point represents m^* averaged over different Landau level filling factors, ν , and the error bars include the variation of m^* with ν . The dashed curves through the data points are guides to the eye.

In contrast, in the present, 4.5 nm-wide AlAs QW, the electrons occupy a single, out-of-plane valley with an isotropic Fermi contour and isotropic $m_b = m_t = 0.205$ [32]. In spite of these differences, our main findings, summarized in Fig. 1, are consistent with the study in Ref. [26]: When the 2DES is partially spin-polarized (open symbols), m^* is larger than its band value and gradually increases with decreasing density. But as we fully

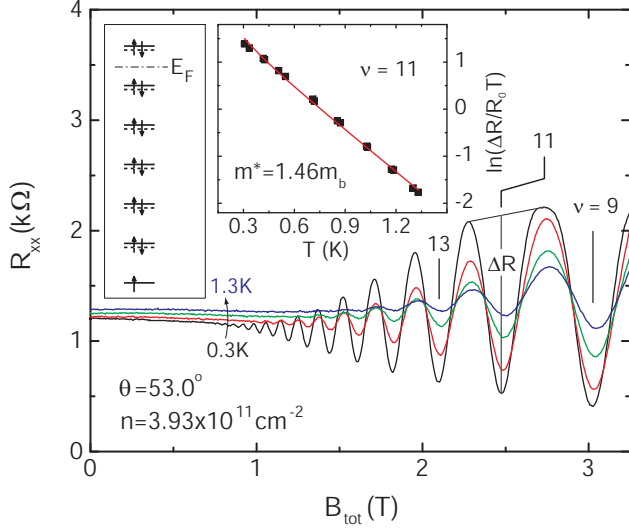


FIG. 2: (Color online) Magneto-resistance traces at a density of $3.93 \times 10^{11} \text{ cm}^{-2}$ and $\theta = 53.0^\circ$. The traces were taken at $T \cong 0.34, 0.71, 1.03$ and 1.30 K. Insets show the energy level diagram at this tilt angle (left) and the Dingle fit at $\nu = 11$ assuming a constant τ_q and R_o (right).

spin polarize the 2DES by subjecting it to strong parallel magnetic fields [33], m^* is suppressed down to values near the band mass (closed symbols). The two colors in Fig. 1 correspond to two different types of analyses used for the m^* determination, which we will discuss later in the paper. Given that this system is close to an ideal 2DES in the sense that it has a very small layer thickness and an isotropic Fermi contour, it appears that mass suppression upon full spin polarization is a genuine property of interacting 2DESs.

We performed measurements on a sample grown on a GaAs (001) substrate and consisting of a 4.5 nm-wide AlAs QW, flanked by $\text{Al}_{0.4}\text{Ga}_{0.6}\text{As}$ barriers [23, 28, 34]. We patterned the sample in a Hall bar configuration, and made ohmic contacts by depositing AuGeNi and alloying in a reducing environment. Metallic front and back gates were deposited to control the carrier density, n , which was determined from the frequency of Shubnikov de Haas (SdH) oscillations and from the Hall resistance. Values of n in our sample are in the range of 1.07 to $4.9 \times 10^{11} \text{ cm}^{-2}$, with mobilities $\mu = 1.4$ to $4.9 \text{ m}^2/\text{Vs}$. Using the AlAs dielectric constant of 10 and the band effective mass $m_b = 0.205$, our density range corresponds to $3.1 < r_s < 6.7$, where r_s is the ratio of the average inter-electron spacing measured in units of the effective Bohr radius. The magneto-resistance measurements were performed down to a temperature (T) of 0.3 K, and up to a magnetic field of 31 T, using low-frequency lock-in techniques. The sample was mounted on a tilting stage to allow the angle, θ , between the normal to the sample and the magnetic field to be varied *in situ*.

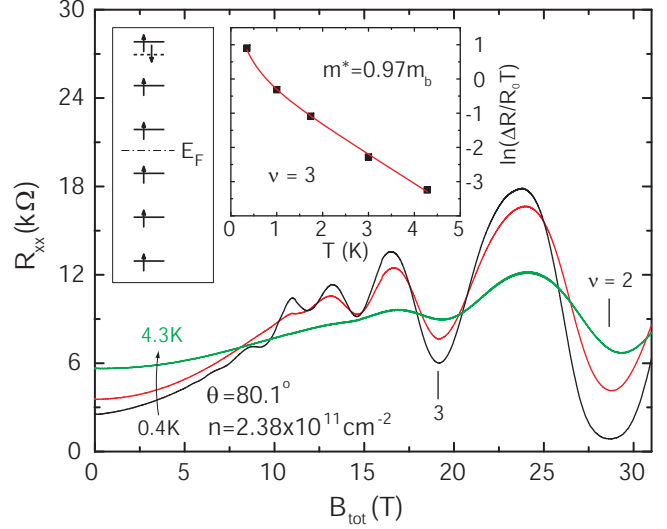


FIG. 3: (Color online) Magneto-resistance traces at a density of $2.38 \times 10^{11} \text{ cm}^{-2}$ and $\theta = 80.1^\circ$. The traces were taken at $T \cong 0.35, 1.74$ and 4.28 K. Insets show the energy level diagram at this tilt angle (left) and the Dingle fit at $\nu = 3$ assuming a constant τ_q and R_o (right).

To deduce m^* , we analyzed the T -dependence of the strength (ΔR) of the SdH oscillations using the standard Dingle expression [35]: $\Delta R/R_o = 8 \exp(-\pi/\omega_c \tau_q) \xi / \sinh(\xi)$, where the factor $\xi / \sinh(\xi)$ represents the T -induced damping ($\xi = 2\pi^2 k_B T / \hbar \omega_c$), and $\omega_c = eB_\perp / m^*$ is the cyclotron frequency, B_\perp is the perpendicular component of the magnetic field, R_o is the non-oscillatory component of the resistance near a SdH oscillation, and τ_q is the single-particle (quantum) lifetime. We analyzed our data using two methods, each based on a different set of assumptions. First, we assumed that both R_o and τ_q are T -independent. This is the usual assumption, commonly made when the T -dependence of R_o is small. For our sample the T -dependence of R_o is indeed weak at high densities (see, e.g., Figs. 2-3). At low densities, however, R_o is T -dependent and, for the lowest densities, R_o changes by as much as 60% in the temperature range of our data (see, e.g., Figs. 4 and 5), implying that τ_q can depend on T . According to a theoretical study [36], for short-range scatterers, the relative T -dependent correction to τ_q is half of the relative correction to the transport scattering time $\tau_{tr} \propto 1/R_o$. For long-range scatterers, the T -dependent correction to τ_q is expected to be smaller [37]. In our second analysis method, we included the T -dependence of R_o , and assumed that the relative T -dependence of τ_q is equal to half the relative T -dependence of R_o [38]. Note that these two methods should bound the maximum error in m^* determination introduced by the T -dependence of τ_q [39].

Figure 2 shows representative data for the partially

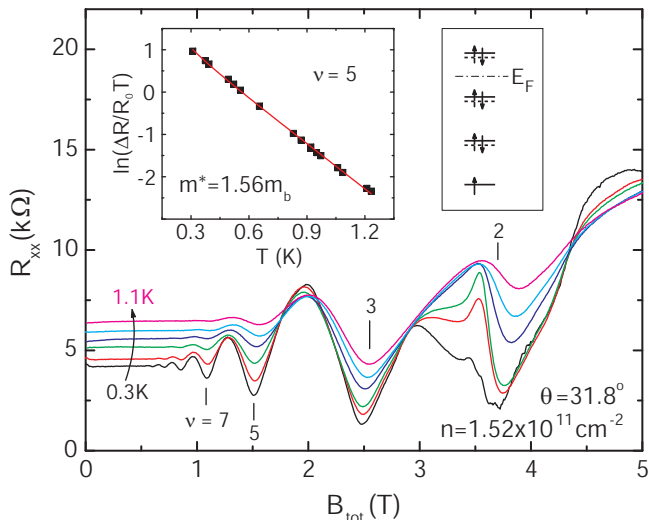


FIG. 4: (Color online) Magneto-resistance traces at a density of $1.52 \times 10^{11} \text{ cm}^{-2}$ and $\theta = 31.8^\circ$. The traces were taken at $T \cong 0.31, 0.49, 0.65, 0.83, 0.95$ and 1.09 K. Insets show the energy level diagram at this tilt angle (right) and the Dingle fit at $\nu = 5$ using a constant τ_q and R_o (left).

spin polarized case at a relatively high density, $n = 3.93 \times 10^{11} \text{ cm}^{-2}$. The angle θ is set carefully so that the opposite spin levels are at coincidence as shown in the left inset of Fig. 2 [40]. Consistent with this energy level diagram, in the magneto-resistance traces shown in Fig. 2, resistance minima at odd ν are strong while the minima at even ν are entirely absent. By fitting the amplitude of the SdH oscillations near $\nu = 11$ to the Dingle expression and assuming T -independent τ_q and R_o , we obtain $m^* = 1.46 m_b$ (see Fig. 2 right inset). Moreover, as illustrated in the Dingle plot in Fig. 6(a), in the whole temperature and magnetic field range the data set can be fit to the Dingle expression by assuming two constants τ_q and m^* . Since the background resistance in this case has a very small temperature dependence, our second analysis method that assumes T -dependent τ_q and R_o yields essentially the same m^* .

In Fig. 3 we show data at the density of $2.38 \times 10^{11} \text{ cm}^{-2}$, at a very high tilt angle, $\theta = 80.1^\circ$. At this θ , the magneto-resistance traces initially show a rise with magnetic field because of the loss of screening with increasing spin polarization [41]. The 2DES becomes fully spin polarized above $B_{tot} \cong 11$ T, and the resistance minima at $2 \leq \nu \leq 5$ are clearly observed. Note that at this angle, the lowest five Landau levels are spin polarized as indicated by the energy level diagram shown in Fig. 3 left inset. To measure the fully spin polarized m^* we fit the amplitude of the SdH oscillations near $\nu = 3$ to the Dingle expression by assuming T -independent τ_q and R_o , and we deduce $m^* = 0.97 m_b$ (see Fig. 3 right inset). As is apparent from the magneto-resistance traces, although

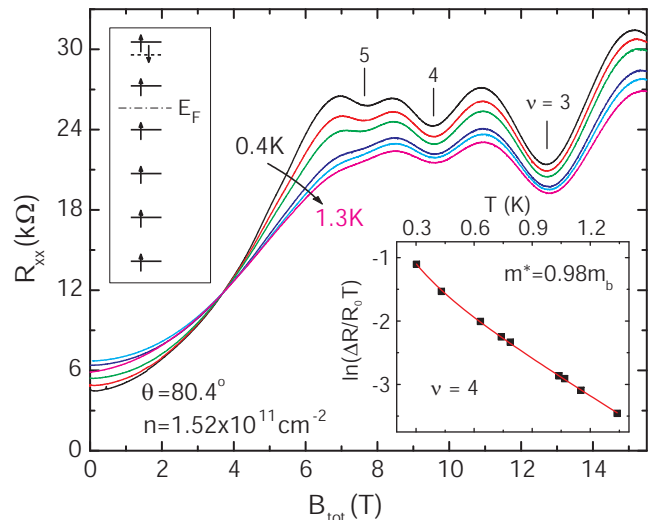


FIG. 5: (Color online) Magneto-resistance traces for the same density as in Fig. 4 at $\theta = 80.4^\circ$. The traces were taken at $T \cong 0.43, 0.63, 0.78, 1.07, 1.15$ and 1.30 K. Insets show the energy level diagram for this tilt angle (left) and the Dingle fit at $\nu = 4$ using a constant τ_q and R_o (right).

at zero field there is a considerable change in resistance with temperature, the background resistance at the SdH oscillation near $\nu = 3$ is small. Therefore including the T -dependence of R_o in the analysis does not make much difference and our first and second analysis methods give essentially identical results.

Now we present data at a lower density ($n = 1.52 \times 10^{11} \text{ cm}^{-2}$) where temperature dependence of the background is strong. Figure 4 shows data for the partially spin polarized case for this density. Consistent with the energy level diagram in the right inset of Fig. 4, θ is set to the coincidence angle so that the resistance minima at odd ν are strong while the minima at even ν are either entirely absent or are accompanied by a spike (e.g., at $\nu = 2$) [42]. By fitting the amplitude of the SdH oscillations near $\nu = 5$ to the Dingle expression and assuming T -independent τ_q and R_o , we obtain $m^* = 1.56 m_b$ (see Fig. 4 left inset). The Dingle plot for this data set is also shown in Fig. 6(b). It is apparent from the quality of the fit that single τ_q and m^* can explain the whole data set in the given temperature and magnetic field range. However, as discussed before, the quality of the fit does not justify the assumption of τ_q being T -independent. In addition, as can be seen from the magneto-resistance traces in Fig. 4, R_o changes with T as much as 50% in the indicated temperature range, implying that τ_q can also be T -dependent. Therefore, applying our second analysis method, i.e., including the T -dependence of R_o and assuming a T -dependent τ_q that changes by 25% in the same temperature range, we deduce $m^* = 1.44 m_b$.

In Fig. 5 we show data at the same density as in Fig. 4

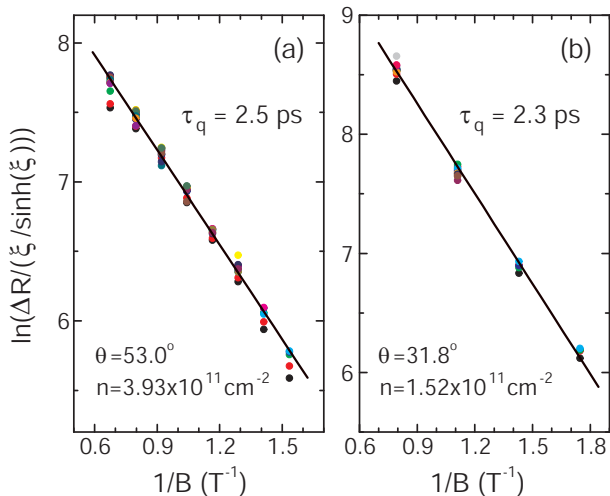


FIG. 6: (Color online) Dingle plots of $\Delta R/(\xi/\sinh(\xi))$ vs. $1/B$ summarizing data taken for the partially spin polarized case for: (a) a density of $3.93 \times 10^{11} \text{ cm}^{-2}$ in the range $0.3 \lesssim T \lesssim 1.3 \text{ K}$ and $11 \leq \nu \leq 25$; and (b) a density of $1.52 \times 10^{11} \text{ cm}^{-2}$ in the range $0.3 \lesssim T \lesssim 1.1 \text{ K}$ and $5 \leq \nu \leq 11$.

but at a very high tilt angle, $\theta = 80.4^\circ$. Main features of the data are the same as in Fig. 3: Magneto-resistance traces show an initial rise with magnetic field and the 2DES becomes fully spin polarized above $B_{tot} \cong 7 \text{ T}$. Filling factors $\nu \leq 5$ are in the fully spin polarized regime as indicated by the energy level diagram shown in Fig. 5 left inset. To measure the fully spin polarized m^* we fit the amplitude of the SdH oscillations near $\nu = 4$ to the Dingle expression by assuming T -independent τ_q and R_o , and we deduce $m^* = 0.98 m_b$ (see Fig. 3 right inset). As can be seen from the magneto-resistance traces, the 2DES goes through a metal-insulator transition at $B_{tot} \cong 3.7 \text{ T}$ before the electrons become fully spin polarized [23]. The background resistance around $\nu = 4$ therefore has an insulating behavior. Again using our second method, i.e., including the T -dependence of R_o and assuming a T -dependent τ_q that is half as large as the T -dependence of R_o , we deduce $m^* = 1.11 m_b$.

We analyzed data at various ν at several densities. Our results are summarized in Fig. 1, where each data point represents m^* averaged over different ν , and the error bar includes the variation of m^* with ν . The results from the first and second analysis methods are shown in black and red in Fig. 1, respectively. At high densities where the background is T -independent, the two methods yield essentially identical results. However, as the density of the 2DES is lowered, the T -dependent background becomes stronger and the two methods give slightly different masses. Independently of the method we use, our conclusions remain the same: In the partially spin polarized case [43] m^* is enhanced over m_b and increases with decreasing density, while for the fully spin polarized

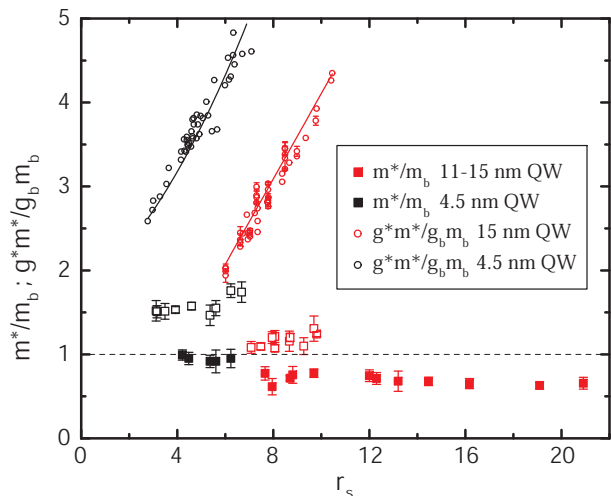


FIG. 7: (Color online) Normalized effective mass and spin susceptibilities of both narrow and wide AlAs QWs as a function of the interaction strength, r_s . Black and red circles are $g^*m^*/g_b m_b$ of 4.5 nm and 15 nm-wide AlAs QWs taken from Refs. [23] and [10], respectively. Open and closed red squares are m^*/m_b for partially and fully spin polarized system, respectively, for 11 to 15 nm-wide AlAs QWs from Ref. [26]. Black squares are m^*/m_b data measured in our sample for a 4.5 nm-wide AlAs QW.

system m^* values are clearly suppressed compared to the partially spin polarized case and are very close to m_b .

As another summary plot, in Fig. 7 we show the normalized effective mass and the spin susceptibilities of both narrow and wide AlAs QWs as a function of interaction strength, r_s . Black and red circles are the normalized spin susceptibilities of 4.5 nm and 15 nm-wide AlAs QWs, taken from Refs. [23] and [10], respectively. Open and closed red squares represent m^*/m_b for partially and fully spin polarized system, respectively, for the wide AlAs QWs of Ref. [26]. Black squares are the measured m^* data for our sample that are shown in Fig. 1.

In an ideal 2DES, the normalized values of the spin susceptibility and effective mass each should follow a universal curve as a function of r_s [3, 9]. However non-ideal factors such as finite layer thickness, anisotropy of the Fermi contour, and disorder give non-universal corrections. Although for high quality samples the effect of disorder is small [4, 5], finite layer thickness and anisotropy of the Fermi contour modify the interaction significantly [5, 6, 10, 44] and change the spin susceptibility and the effective mass renormalization. Because of the small layer thickness and isotropic Fermi contour of the electrons in narrow AlAs samples, the spin susceptibility follows very closely the predictions of quantum Monte Carlo calculations for an ideal 2D system (not shown) [3, 5, 23, 28]. However, for wide AlAs samples the measured susceptibilities are considerably lower than narrow AlAs samples

because the strength of the Coulomb interaction is reduced by the finite layer thickness effect [5, 6] and the anisotropy of the Fermi contour [10]. It is clear from the data that the partially spin polarized masses for wide AIAs QWs are also smaller than for narrow AIAs QWs even though the r_s values are larger. Similar to the spin susceptibility case [10], the corrections to m^* due to the layer thickness and the anisotropic effective mass are expected to give smaller m^* values in the partially spin polarized case [6, 9], consistent with our data. In addition, we emphasize that the mobility of the electrons in narrow quantum wells are much lower compared to wide quantum wells because of the prevalence of the interface roughness scattering. Therefore, it is also possible that the higher disorder in narrow quantum wells is responsible for m^* being larger [4]. We point out that in the partially polarized case there are also some quantitative differences between our results on narrow AIAs QWs and the previous studies done on Si-MOSFETs [17, 18, 19] and GaAs 2DESs [24]. It has been reported that in GaAs 2DESs m^* has a strong r_s dependence although m^* values are much smaller compared to narrow AIAs QWs for the similar r_s range. It is likely that this discrepancy is because of the larger finite layer thickness and less disorder in 2DESs in GaAs samples. On the other hand, because of the valley degeneracy of Si-MOSFET samples, such a comparison is not valid: as shown in Ref. [27], the valley degeneracy affects the mass renormalization considerably.

In the fully polarized regime, it is natural to also expect some dependence of m^* on the layer thickness, Fermi contour anisotropy and disorder. However, it is not clear from the data whether m^* are lower for wide AIAs samples because of non-ideal factors or because these masses are measured at larger r_s values. We conclude that the mass suppression is very robust and is observed in a very wide range of r_s values and independent of sample and system parameters such as disorder, layer thickness and anisotropy.

It is intuitively clear that, the spin polarization of the 2DES should affect the m^* re-normalization since it modifies the exchange interaction. Naively, one might think that for a fully spin polarized system the Fermi energy is doubled so the interaction is weaker compared to the spin unpolarized case, and hence the mass for the spin polarized case would be smaller. Although this argument gives the correct qualitative behavior of m^* for a fixed density, it does not explain why m^* for the fully polarized system stays small (near or below m_b) even at very high r_s values. Recent theoretical work [7, 8] has addressed the role of spin-polarization on m^* re-normalization. It is reported in Ref. [7] that m^* very weakly depends on the spin polarization for valley degenerate systems. Since in our case the 2D electrons occupy a single valley, this is not relevant to our data. The more relevant study [8], which deals with a single-valley system, reports a

rather strong dependence of m^* on the degree of spin-polarization. Although it is predicted in Ref. [8] that for a fully spin-polarized 2DES m^* is smaller compared to the spin unpolarized case, there remains major qualitative discrepancies with our data. For example, m^* for a fully spin polarized system is predicted to increase with increasing r_s and become smaller than m_b only for $r_s < 2$. In contrast, our data suggest that m^* stays very close to m_b even in the range $4 < r_s < 6$. Including the data from Ref. [26], which extends up to $r_s \simeq 21$, the discrepancy becomes even more serious. An understanding of the magnitude and density dependence of m^* for a single component (single valley and fully spin polarized) 2DES awaits future theoretical developments.

In summary, we confirmed the observation of m^* suppression upon full spin polarization in a system with a very small layer thickness and isotropic Fermi contour. Since this system is very close to an ideal 2DES, our data suggest that mass suppression for a single component system is a general property of an interacting 2DES.

We thank the NSF for support. Part of this work was done at the NHMFL, Tallahassee, which is also supported by the NSF. We thank E. Palm, T. Murphy, B. Pullum and S. Maier for assistance.

-
- [1] B. Tanatar and D.M. Ceperley, Phys. Rev. B **39**, 5005 (1989).
 - [2] Y. Kwon, D.M. Ceperley, and R.M. Martin, Phys. Rev. B **50**, 1684 (1994).
 - [3] C. Attacalite, S. Moroni, P. Gori-Giorgi, and G.B. Bachelet, Phys. Rev. Lett. **88**, 256601 (2002).
 - [4] R. Asgari, B. Davoudi, and B. Tanatar Solid State Commun. **130**, 13 (2004).
 - [5] S. De Palo, M. Botti, S. Moroni, and G. Senatore, Phys. Rev. Lett. **94**, 226405 (2005).
 - [6] Y. Zhang and S. Das Sarma, Phys. Rev. B. **72**, 075308 (2005).
 - [7] S. Gangadharaiah and D.L. Maslov, Phys. Rev. Lett. **95**, 186801 (2005).
 - [8] Y. Zhang and S. Das Sarma, Phys. Rev. Lett. **95**, 256603 (2005).
 - [9] R. Asgari and B. Tanatar, Phys. Rev. B **74**, 075301 (2006).
 - [10] T. Gokmen, M. Padmanabhan, E. Tutuc, M. Shayegan, S. De Palo, S. Moroni, and G. Senatore, Phys. Rev. B **76**, 233301 (2007).
 - [11] F.F. Fang and P.J. Stiles, Phys. Rev. **174**, 823 (1968).
 - [12] J.L. Smith and P.J. Stiles, Phys. Rev. Lett. **29**, 102 (1972).
 - [13] T. Okamoto, K. Hosoya, S. Kawaji, and A. Yagi, Phys. Rev. Lett. **82**, 3875 (1999).
 - [14] W. Pan, D.C. Tsui, and B.L. Draper, Phys. Rev. B **59**, 10208 (1999).
 - [15] S.A. Vitkalov, H. Zheng, K.M. Mertes, M.P. Sarachik, and T.M. Klapwijk, Phys. Rev. Lett. **87**, 086401 (2001).
 - [16] A.A. Shashkin, S.V. Kravchenko, V.T. Dolgoplov, and T.M. Klapwijk, Phys. Rev. Lett. **87**, 086801 (2001).

- [17] A.A. Shashkin, S.V. Kravchenko, V.T. Dolgoplov, and T.M. Klapwijk, Phys. Rev. B **66**, 073303 (2002).
- [18] V.M. Pudalov, M.E. Gershenson, H. Kojima, N. Butch, E.M. Dizhur, G. Brunthaler, A. Prinz, and G. Bauer, Phys. Rev. Lett. **88**, 196404 (2002).
- [19] A.A. Shashkin, Maryam Rahimi, S. Anissimova, S.V. Kravchenko, V.T. Dolgoplov, and T.M. Klapwijk, Phys. Rev. Lett. **91**, 046403 (2003).
- [20] J. Zhu, H.L. Stormer, L.N. Pfeiffer, K.W. Baldwin, and K.W. West, Phys. Rev. Lett. **90**, 056805 (2003).
- [21] O. Prus, Y. Yaish, M. Reznikov, U. Sivan, and V. Pudalov, Phys. Rev. B **67**, 205407 (2003).
- [22] E. Tutuc, S. Melinte, E.P. De Poortere, M. Shayegan, and R. Winkler, Phys. Rev. B **67**, 241309(R) (2003).
- [23] K. Vakili, Y.P. Shkolnikov, E. Tutuc, E.P. De Poortere, and M. Shayegan, Phys. Rev. Lett. **92**, 226401 (2004).
- [24] Y.-W. Tan, J. Zhu, H.L. Stormer, L.N. Pfeiffer, K.W. Baldwin, and K.W. West, Phys. Rev. Lett. **94**, 016405 (2005).
- [25] Y.-W. Tan, J. Zhu, H.L. Stormer, L.N. Pfeiffer, K.W. Baldwin, and K.W. West, Phys. Rev. B **73**, 045334 (2006).
- [26] M. Padmanabhan, T. Gokmen, N.C. Bishop, and M. Shayegan, Phys. Rev. Lett. **101**, 026402 (2008).
- [27] T. Gokmen, M. Padmanabhan, and M. Shayegan, Phys. Rev. Lett. **101**, 146405 (2008).
- [28] M. Shayegan, E.P. De Poortere, O. Gunawan, Y.P. Shkolnikov, E. Tutuc, K. Vakili, Phys. Stat. Sol. (b) **243**, 3629 (2006).
- [29] T.S. Lay, J.J. Heremans, Y.W. Suen, M.B. Santos, K. Hirakawa, M. Shayegan, and A. Zrenner, Appl. Phys. Lett. **62**, 3120 (1993).
- [30] H. Momose, N. Moria, C. Hamaguchia, T. Ikaidab, H. Arimoto and N. Miura, Physica E 4, 286 (1999).
- [31] O. Gunawan, E. P. De Poortere, and M. Shayegan, Phys. Rev. B **75**, 081304(R) (2007).
- [32] We use $m_b = m_t = 0.205 \pm 0.005$ for the out-of-plane valley, based on values reported in different studies of either the cyclotron resonance or the ballistic transport measurements (Refs. [29, 30, 31]).
- [33] In a 2DES with finite electron layer thickness, parallel magnetic couples to the orbital motion of the electrons and leads to an increase of m^* [T. Gokmen, M. Padmanabhan, O. Gunawan, Y.P. Shkolnikov, K. Vakili, E.P. DePoortere, and M. Shayegan, Phys. Rev. B **78**, 233306 (2008)]. However because of the very small electron layer thickness in our narrow quantum well, we expect that the mass enhancement is less than 5% even at $B_{\parallel} = 30$ T.
- [34] K. Vakili, Y.P. Shkolnikov, E. Tutuc, E.P. De Poortere, M. Padmanabhan, and M. Shayegan, Appl. Phys. Lett. **89**, 172118 (2006).
- [35] R.B. Dingle, Proc. R. Soc. London A **211**, 517 (1952).
- [36] Y. Adamov, I.V. Gornyi, and A.D. Mirlin, Phys. Rev. B **73**, 045426 (2006).
- [37] S. Das Sarma, unpublished
- [38] We emphasize that in all cases our data can be fit reasonably well to the Dingle expression in the whole temperature and magnetic field range by assuming two constants τ_q and m^* (see, e.g., Fig. 6). However, this does not justify that τ_q is independent of T ; indeed a given data set can be fit equally well to the Dingle expression with a different, fixed m^* , and a τ_q that has some T -dependence. Since m^* and the T -dependence of τ_q cannot be determined independently, in our second analysis method we use the T -dependence of the background resistance to estimate the T -dependence of $1/\tau_q$ and deduce m^* .
- [39] Although the T -dependence of R_o and τ_q tend to cancel each other in the fitting of m^* , it is the T -dependence of τ_q that dominates since τ_q appears inside the exponential term.
- [40] The partially spin polarized masses are also reported in Ref. [23]. However those masses are not deduced at the coincidence condition. Setting the coincidence condition is important because when the spin-up and spin-down levels do not overlap, the gap is smaller than the cyclotron energy and one may get artificially larger values for m^* .
- [41] V.T. Dolgoplov and A. Gold, JETP Lett. **71**, 27 (2000); I.F. Herbut, Phys. Rev. B **63**, 113 102 (2001).
- [42] E.P. De Poortere, E. Tutuc, S.J. Papadakis, M. Shayegan, Science **290**, 1546 (2000).
- [43] In our study, the partially-spin-polarized regime corresponds to spin polarization ranging from 4% to 20%.
- [44] In 2D systems the nonuniversal correction arising from the finite layer thickness is a conceptually simple form-factor that modifies the bare Coulomb interaction. Similarly, the Fermi contour anisotropy can be incorporated in Coulomb interaction by making a coordinate transformation that makes the Fermi surface isotropic but the interactions anisotropic.